Weak lensing effects in the measurement of the dark energy equation of state with LISA

Chris Van Den Broeck,[1,2,*] M. Trias,[3,†] B. S. Sathyaprakash,[2,‡] and A. M. Sintes[3,§]

[1]*Nikhef, National Institute for Subatomic Physics, Science Park 105, 1098 XG Amsterdam, The Netherlands*
[2]*School of Physics and Astronomy, Cardiff University, Queen's Buildings, The Parade, Cardiff, CF24 3AA, United Kingdom*
[3]*Departament de Física, Universitat de les Illes Balears, Carretera Valldemossa Km. 7.5, E-07122 Palma de Mallorca, Spain*

The Laser Interferometer Space Antenna's (LISA's) observation of supermassive binary black holes (SMBBH) could provide a new tool for precision cosmography. Inclusion of subdominant signal harmonics in the inspiral signal allows for high-accuracy sky localization, dramatically improving the chances of finding the host galaxy and obtaining its redshift. A SMBBH merger can potentially have component masses from a wide range (10^5–$10^8 M_\odot$) over which parameter accuracies vary considerably. We perform an in-depth study in order to understand (i) what fraction of possible SMBBH mergers allow for sky localization, depending on the parameters of the source, and (ii) how accurately w can be measured when the host galaxy can be identified. We also investigate how accuracies on all parameters improve when a knowledge of the sky position can be folded into the estimation of errors. We find that w can be measured to within a few percent in most cases, if the only error in measuring the luminosity distance is due to LISA's instrumental noise and the confusion background from Galactic binaries. However, weak lensing-induced errors will severely degrade the accuracy with which w can be obtained, emphasizing that methods to mitigate weak lensing effects would be required to take advantage of LISA's full potential.

I. INTRODUCTION

The Laser Interferometer Space Antenna (LISA) is a space-based gravitational-wave detector that can observe the merger of supermassive black holes in a binary with signal-to-noise ratios (SNRs) of hundreds to thousands. So far, it has not been possible to predict the rate of mergers in the Universe, and the event rate for LISA, with any precision. The initial seed black holes could have masses anywhere in the range $\sim 100 - 10^5 M_\odot$, depending on the formation scenario. Collapse of metal-free massive stars at $z \gtrsim 20$ could lead to *light* seeds, with masses of a few hundred solar masses [1]. On the other hand, gravitational instability of massive proto-galactic disks could lead to the formation at $z \gtrsim 10$ of *heavy* seeds with masses $\sim 10^5 M_\odot$ [2]. These black hole seeds might grow by *prolonged* accretion whereby infalling matter has a constant angular momentum direction and spins up the black hole [3,4]. Alternatively, the seeds might grow by chaotic accretion associated with sporadic infall of small amounts of matter from a fragmented disc [5]. The merger history in LISA's past light cone depends on how black holes formed and evolved. If seed black holes were heavy, then one expects several tens of mergers per year, and LISA will observe all of them. If the seeds were small, then the rate in LISA's past light cone could be 2 to 3 times larger, but LISA's sensitivity to smaller black holes will be poorer, and the number of mergers observed is again a few tens per year.

Of these, a handful of events might be close enough to be useful for cosmography [6].

LISA may open a new era for precision cosmography since black hole binaries are *self-calibrating standard sirens* [7–9]. In astronomy, a standard candle is a source whose absolute luminosity can be deduced from certain observed properties such as the time variability of its light curve, spectral characteristics, etc. Analogously, the term *standard siren* is used for binary black holes, since the way gravitational waves interact with matter is more akin to sound waves, although, of course, they are transverse waves traveling at the speed of light. Black holes are also *self-calibrating* since they do not need other measures of distance to calibrate their luminosity. This is because the luminosity of a binary black hole depends only on its chirp mass[1] and its luminosity distance from LISA. For a chirping binary, i.e., a binary whose gravitational-wave frequency changes by an observable amount during the course of observation, one can deduce the chirp mass and measure its amplitude and thereby infer its luminosity distance. Therefore, binary black holes can provide a new calibration for the high redshift Universe avoiding all the lower rungs of the cosmic distance ladder.

Supermassive binary black hole (SMBBH) mergers are, therefore, potential tools for cosmology. Indeed, a single SMBBH observation by LISA might already significantly constrain the dark energy equation-of-state parameter w [8–11]. From the gravitational waveform, one obtains the luminosity distance, D_L. Because of LISA's orbital motion

---

*vdbroeck@nikhef.nl
†miquel.trias@uib.es
‡B.Sathyaprakash@astro.cf.ac.uk
§alicia.sintes@uib.es

---

[1]The chirp mass $\mathcal{M}$ of a binary of total mass M and reduced mass μ is $\mathcal{M} = \mu^{3/5} M^{2/5}$.

over the observation time, one can also obtain an approximate sky position. If this allows for localization of the host galaxy, then redshift z can be measured. Since the relationship between D_L and z depends sensitively on w (among other cosmological parameters), the latter can then be constrained. One of the hurdles in availing of LISA for cosmology was that LISA's angular resolution might not be good enough to localize the host galaxy—a step that is crucial for obtaining the redshift of the source. However, more recent work has mitigated this hurdle by showing that the use of the full signal waveform, which contains not only the dominant harmonic at twice the orbital frequency $2f_{orb}$, but also other harmonics kf_{orb}, $k = 1, 3, 4, \ldots$, in parameter estimation can improve the angular resolution to a level that enables the localization of the source for a large fraction of systems in LISA's band [10–14]. The subdominant harmonics, therefore, are essential for precision cosmology with LISA.

The above conclusions have mainly been drawn by computing the covariance matrix of the intrinsic and extrinsic parameters associated with an SMBBH. A binary consisting of nonspinning black holes on a quasicircular orbit is characterized by nine parameters: the chirp mass $\mathcal{M}$ and reduced mass μ, a radial vector $(D_L, \theta_N, \varphi_N)$ giving the location of the source, the orientation of the angular momentum (θ_L, φ_L) at a fiducial time, the epoch of merger t_C, and the signal's phase φ_C at that epoch. The information matrix (inverse of the covariance matrix) tends to be rather ill-conditioned, and it is necessary to exercise a lot of care in its computation and inversion. Several groups have independently confirmed the measurement accuracies, and it is now widely believed that subdominant harmonics truly bring about a dramatic improvement in the estimation of parameters [6,10–17]. One of the implications is that LISA will be able to measure the masses of the component black holes very accurately and obtain the mass function of (seed) black holes.

Localizing the source well enough for its host galaxy to be identified is crucial for measuring w, since a knowledge of the redshift is needed. One may then ask how parameter estimation in general benefits from a knowledge of the sky position. In the full nine-dimensional parameter space, θ_N and ϕ_N are partially correlated with the other seven parameters. The associated degeneracies in parameter estimation get broken if (θ_N, ϕ_N) are exactly known. The covariance matrix then gets reduced from a 9×9 to a 7×7 matrix, leading to smaller uncertainties [11,18].

In Refs. [10,11], it was shown how the inclusion of subdominant signal harmonics allows for a sufficiently good localizability of the source in the sky and measurement of the luminosity distance that inference of w becomes possible. However, in those papers only a limited number of possible parameter values were considered. The event rates mentioned above are integrated over a large range of masses, and it is important to know how accurately LISA can measure w, depending on which binaries it observes during its lifetime; indeed, the quality of parameter estimation varies widely depending on the properties of the sources [12–14]. Here, we report on an exhaustive study of the relevant part of parameter space. We look at 15 mass pairs with (observed) component masses roughly in the range 10^5–$10^8 M_\odot$, at a fixed redshift. For each of these, a Monte Carlo (MC) simulation is performed with 5000 instances of sky position and orientation of the orbital plane. We then compute in what percentage of these cases one would be able to estimate sky position well enough that host identification should be possible. Using only these instances, we calculate the distribution of the uncertainties in w. Our Monte Carlo results are in such a form that they allow for easy rescaling to different redshifts z; we study what happens at $z = 0.55$, $z = 0.7$, and $z = 1$. LISA's instrumental noise will not be the only restriction in the measurement of w; weak lensing will affect the determination of luminosity distance. To assess weak lensing effects, our distance errors are combined in quadrature with a 4% additional error due to weak lensing [19].

This paper is structured as follows: In Sec. II, we give a brief description of the signal model used in our study. Our choice of systems is explained in Sec. III, and we study the impact of source localizability on parameter estimation in Sec. IV. In Sec. V, we describe how we go about determining the dark energy parameter w, including our criteria for localizability of the source. In Sec. VI, we discuss the results of our study, giving the fraction of systems for which the host galaxy can be localized, and the level at which w can be estimated, depending on what kind of system is observed. We will show that weak lensing-induced errors in D_L will severely limit LISA's ability to measure w. We conclude in Sec. VII with the message that future studies should focus on correcting the effect of weak lensing.

Throughout this paper we set $G = c = 1$ unless stated otherwise.

II. SIGNAL MODEL AND LISA CONFIGURATION

The coalescence of black hole binary systems is commonly divided into three successive epochs: inspiral, merger, and ringdown. During the inspiral, the two black holes are well separated, and the radial inspiral time scale is much larger than the orbital time scale. As a consequence, the gravitational-wave signal emitted during this regime is well-understood analytically, in terms of the post-Newtonian (PN) approximation of general relativity. The latter is a perturbative approach whereby the amplitudes and phases of gravitational waveforms are expressed in terms of a characteristic velocity v (see [20] and the extensive references therein). The dynamics of the binary system will be modeled very well in this way for many orbits, but eventually there comes a point where the PN approximation fails; after that a numerical solution to the

full Einstein equations is called for. This happens when the *innermost stable circular orbit* (ISCO) is reached, after which the black holes plunge towards each other to form a single black hole; this is referred to as the merger phase of the coalescence. The resulting black hole then undergoes "ringdown" as it gradually settles down to a quiescent Kerr black hole.

Although most of the SNR is accumulated during the final stages of inspiral and merger, disentangling the parameters that characterize the system and extracting physical information relies critically on longer observation times, so that it is important to carefully study the inspiral phase. In this work we focus on LISA parameter estimation from observations of just the inspiral process. By doing so we can make use of analytical expressions for the detector response and its derivatives with respect to the different parameters which are needed to perform parameter estimation. This allows us to implement fast algorithms and explore the parameter space in a comprehensive way, unlike in numerical simulations where one can only consider a single choice of parameters (masses, spins, ...) at a time. In this way we are able to carry out an extensive study of LISA's performance, in particular, in measuring the dark energy equation of state. Nevertheless, by not including the merger and ringdown we are missing a fraction of the total SNR that LISA would observe (especially for the higher mass systems), which would improve parameter estimation. While there has been recent work on parameter estimation with LISA using numerical waveforms that include merger and ringdown [21,22], some more understanding may be needed before embarking on extensive studies (but see the semi-analytic approach of [23]). As far as inspiral itself is concerned, Stavridis *et al.* [24] studied the effect of spin-induced precession of the orbital plane on our ability to measure w, though without inclusion of higher signal harmonics in the waveform. The work presented here is complementary, in that it assumes zero spins but does include higher harmonics in the analysis.

The inspiral PN waveforms in the two polarizations h_+ and $h_\times$ take the general form

$$h_{+,\times} = \frac{2M\nu}{D_L}(M\omega)^{2/3}\{H_{+,\times}^{(0)} + x^{1/2}H_{+,\times}^{(1/2)} + xH_{+,\times}^{(1)}$$
$$+ x^{3/2}H_{+,\times}^{(3/2)} + x^2H_{+,\times}^{(2)} + x^{5/2}H_{+,\times}^{(5/2)} + x^3H_{+,\times}^{(3)}\}.$$
(2.1)

Here, $x(t) \equiv [2\pi MF(t)]^{2/3}$ is the post-Newtonian expansion parameter, with $F(t)$ the instantaneous orbital frequency; $\mathcal{O}(x^q)$ is referred to as qth PN order. For observed component masses m_1 and m_2, $M = m_1 + m_2$ and $\nu = m_1 m_2/M^2$ are, respectively, the observed total mass and the symmetric mass ratio, and D_L is the luminosity distance to the source. The explicit expressions for $H_{+,\times}^{(i/2)}$ up to 3PN can be found in [25]. We neglect the contribution of spins, so that the gravitational waveform

can be parametrized by nine parameters: luminosity distance, D_L; two angles (ϕ_N, θ_N) defining the source position; another two angles (θ_L, ϕ_L) specifying the orientation of the orbital angular momentum; two mass parameters; the phase at coalescence, φ_C; and the time of coalescence, t_C. The sky position and orientation angles are defined with respect to a solar system barycentric frame, as in [26].

For LISA observation of supermassive black hole binary inspirals, most of the SNR accumulates at frequencies below 10 mHz, in which case it is appropriate to use the low-frequency approximation to the LISA response function [26]. In this approximation the detector can be regarded as two independent Michelson interferometers, and the measured strain in each of these separately can be written as

$$h^{(i)}(t) = \frac{\sqrt{3}}{2}[F_+^{(i)}(t)h_+(t) + F_\times^{(i)}(t)h_\times(t)], \quad (2.2)$$

where $i = I, II$ labels the two independent interferometers. The response functions $F_+^{(i)}$ and $F_\times^{(i)}$ depend on time through the sky position and orientation of the source with respect to LISA, which vary over the observation time because of LISA's orbital motion. The factor $\sqrt{3}/2$ is due to the 60° angle between the interferometers' arms.

It is convenient to express the waveform in the Fourier domain using the stationary phase approximation [27]. The Fourier transform $\tilde{h}^{(i)}(f)$ of the response of detector i then takes the form [10,12]

$$\tilde{h}^{(i)}(f) = \frac{\sqrt{3}}{2}\frac{2M\nu}{D_L}$$
$$\times \sum_{k=1}^{8}\sum_{n=0}^{6}\frac{A_{(k,n/2)}^{(i)}(t(f_k))x^{(n/2)+1}(t(f_k))e^{-i\phi_{(k,n/2)}^{(i)}(t(f_k))}}{2\sqrt{k\dot{F}(t(f_k))}}$$
$$\times \exp[i\psi_{f,k}(t(f_k))], \quad (2.3)$$

where $f_k \equiv f/k$, an overdot denotes the derivative with respect to time, and $\psi_{f,k}(t(f_k))$ is given by

$$\psi_{f,k}(t(f_k)) = 2\pi f t(f_k) - k\Psi(t(f_k)) - k\phi_D(t(f_k)) - \pi/4.$$
(2.4)

The waveform is a superposition of harmonics of the orbital frequency (labeled by the index k), and each harmonic has PN contributions to the amplitude (labeled by n; note that currently one can only go up to $n = 6$, as no amplitude corrections are explicitly known beyond 3PN [25]). As the PN order in amplitude is increased, more and more harmonics appear; at 3PN order there are eight, which is why the index k only runs up to $k = 8$. Quantities in Eqs. (2.3) and (2.4) with the argument $t(f_k)$ denote their values at the time when the instantaneous orbital frequency $F(t)$ sweeps past the value f/k. $A_{(k,n/2)}^{(i)}(t)$ and $\phi_{(k,n/2)}^{(i)}(t)$ are the polarization amplitudes and phases of the kth harmonic appearing at $n/2$th PN

order. $\Psi(t)$ is the orbital phase of the binary and $\phi_D(t)$ is a time-dependent term representing Doppler modulation due to LISA's motion around the Sun. Explicit expressions for $A^{(i)}_{(k,n/2)}$ and $\phi^{(i)}_{(k,n/2)}$ can be found in [28,29]; time dependence of these quantities arises through the beam pattern functions due to the varying sky position and orientation of the source relative to the detector [26]. The expression for $\phi_D(t)$ is given in [26]. For the PN expansions for $t(f)$, $\Psi(t)$, $F(t)$, and $\dot{F}(t)$ we refer to [30].

Each harmonic in $\tilde{h}_{(i)}(f)$ is taken to be zero outside a certain frequency range. The upper cutoff frequencies are dictated by the ISCO, beyond which the PN approximation breaks down. For simplicity we assume that this occurs when the orbital frequency $F(t)$ reaches F_{ISCO}, the orbital frequency at ISCO of a test particle in Schwarzschild geometry[2]: $F_{\text{ISCO}} = (6^{3/2}2\pi M)^{-1}$. Consequently, in the frequency domain, the contribution to $\tilde{h}^{(i)}(f)$ from the kth harmonic is set to zero for frequencies above kF_{ISCO}. Thus, the kth harmonic ends at a frequency

$$F^{(k)}_{\text{ISCO}} = 2.198 \times 10^{-3} k \left(\frac{10^6 M_\odot}{M}\right) \text{Hz}. \quad (2.5)$$

In determining the lower cutoff frequencies we assume that the source is observed for at most 1 yr, and the kth harmonic is truncated below a frequency kF_{in}, where F_{in} is the value of the orbital frequency 1 yr before ISCO is reached [10]:

$$F_{\text{in}} = F(t_{\text{ISCO}} - \Delta t_{\text{obs}}) = \frac{F_{\text{ISCO}}}{(1 + \frac{256\nu}{5M}\Delta t_{\text{obs}} v^8_{\text{ISCO}})^{3/8}}. \quad (2.6)$$

For simplicity, F_{in} was computed using the quadrupole formula. In the above, t_{ISCO} and $v_{\text{ISCO}} = 1/\sqrt{6}$ are, respectively, the time and orbital velocity at the last stable orbit, and $\Delta t_{\text{obs}} = 1$ yr. However, LISA's sensitivity becomes poorer and poorer as one goes to lower frequencies, and current estimates normally assume a "noise wall" at a frequency no lower than $f_s = 10^{-5}$ Hz. Thus, we take the lower cutoff frequency of the kth harmonic to be the maximum of f_s and kF_{in}.

As has been shown by several groups, both for Earth-based detectors [28,29] and for LISA [10,12–17,31], taking into account all the harmonics significantly improves the parameter estimation, and at the same time it extends the mass reach to higher mass systems. However, in our computer code we have restricted ourselves to 2PN order in both amplitude and phase. We emphasize that there is no technical difficulty in going to higher orders, but as shown

in [10–13,29], the main improvement in parameter estimation occurs in going from 0PN to 0.5PN order in amplitude, and 2PN order will be more than sufficient for our purposes.

Because of the large SNR values that will be measured by LISA in observing SMBBH events, the Fisher information matrix formalism can be used to perform the parameter estimation. In the limit of high SNR, the probability density distribution of the true parameters near the measured value can be approximated by a multivariate Gaussian distribution whose covariance matrix is given by the inverse of the Fisher information matrix [32]. For each of the interferometers $i = I$, II, the Fisher matrix takes the form

$$\Gamma^{(i)}_{\alpha\beta} \equiv (\partial_\alpha h^{(i)} | \partial_\beta h^{(i)})$$
$$= 2 \int_0^\infty \frac{\partial_\alpha \tilde{h}^{(i)*}(f)\partial_\beta \tilde{h}^{(i)}(f) + \partial_\alpha \tilde{h}^{(i)}(f)\partial_\beta \tilde{h}^{(i)*}(f)}{S_n(f)} df, \quad (2.7)$$

where $\partial_\alpha \equiv \partial/\partial\lambda^\alpha$, with λ^α the parameters to be estimated. Specifically, we take these to be

$$\bar{\lambda} = (t_C, \phi_C, \cos(\theta_N), \phi_N, \cos(\theta_L), \phi_L, \ln D_L, \mathcal{M}, \mu). \quad (2.8)$$

The Fisher matrix for LISA as a whole is then

$$\Gamma_{\alpha\beta} = \Gamma^I_{\alpha\beta} + \Gamma^{II}_{\alpha\beta}. \quad (2.9)$$

The covariance matrix is $\Sigma^{\alpha\beta} = (\Gamma^{-1})^{\alpha\beta}$, which gives the covariances between parameters,

$$\langle \delta\lambda^\alpha \delta\lambda^\beta \rangle = \Sigma^{\alpha\beta}, \quad (2.10)$$

and hence also the 1-σ uncertainties,

$$\Delta\lambda^\alpha \equiv [\langle (\delta\lambda^\alpha)^2 \rangle]^{1/2} = \sqrt{\Sigma^{\alpha\alpha}}, \quad (2.11)$$

where no summation over repeated indices is assumed.

As mentioned above, we use the stationary phase approximation to the gravitational waveform in the frequency domain, which provides a way of getting analytical expressions for the observed signals, $\tilde{h}^{(i)}(f)$, and for their derivatives with respect to the parameters, $\partial_\alpha \tilde{h}^{(i)}(f)$ [10,12]. Only the final integral over f in Eq. (2.7) needs to be done numerically.

The code we use to generate our results has been validated by the LISA Parameter Estimation (LISA PE) Taskforce [33] through cross checking of the output with different codes from other groups [6].

In Eq. (2.7), $S_n(f)$ is the one-sided noise power spectral density, which is a combination of instrumental and galactic confusion noise. We take our noise curve to be the one that was used by all the members of the LISA PE Taskforce in [6], which also corresponds to the noise curve from the second round of the Mock LISA Data Challenges [34,35]. The sky-averaged instrumental noise is defined by

---

[2]Note that the cutoff is placed on the orbital frequency of the binary, not on the dominant harmonic in the gravitational-wave signal, hence, the extra factor of 2 in the denominator of the expression for F_{ISCO} compared to what one often finds in other literature.

$$S_{\text{inst}}(f) = \frac{1}{L^2}\left\{\left[1 + \frac{1}{2}\left(\frac{f}{f_*}\right)^2\right]S_p\right.$$
$$\left. + \left[1 + \left(\frac{0.1 \text{ mHz}}{f}\right)^2\right]\frac{4S_a}{(2\pi f)^4}\right\}, \quad (2.12)$$

where f is in Hz, $L = 5 \times 10^9$ m is the arm length, $S_p = 4 \times 10^{-22}$ m^2 Hz^{-1} is the (white) position noise level, $S_a = 9 \times 10^{-30}$ m^2 s^{-4} Hz^{-1} is the white acceleration noise level and $f_* = c/(2\pi L)$ is the LISA arm transfer frequency (see Ref. [6] for further comments and details).

The galactic confusion noise is estimated by simulating the population synthesis of galactic binaries with periods shorter than 2×10^{-4} s [36,37]. The confusion noise at the output can be fitted as [38]

$$S_{\text{conf}}(f) = \begin{cases} 10^{-44.62}f^{-2/3}, & f \leq 10^{-3} \text{ Hz} \\ 10^{-50.92}f^{-4.4}, & 10^{-3} \text{ Hz} < f \leq 10^{-2.7} \text{ Hz} \\ 10^{-62.8}f^{-8.8}, & 10^{-2.7} \text{ Hz} < f \leq 10^{-2.4} \text{ Hz} \\ 10^{-89.68}f^{-20}, & 10^{-2.4} \text{ Hz} < f \leq 10^{-2} \text{ Hz} \\ 0, & f > 10^{-2} \text{ Hz} \end{cases}$$
$$(2.13)$$

The total noise curve is the sum of instrumental and confusion noise,

$$S_n(f) = S_{\text{inst}}(f) + S_{\text{conf}}(f). \quad (2.14)$$

Finally, as in [6], we also apply a lower frequency cutoff at 10^{-5} Hz.

III. CHOICE OF SYSTEMS STUDIED

LISA's sensitivity band stretches from 10^{-5} Hz to 0.1 Hz, which means [see Eq. (2.5)] that LISA will be able to see the coalescence of SMBBH systems of (observed) total mass from $\sim 10^5 M_\odot$ to $\sim 10^8 M_\odot$ with signal-to-noise ratios of several hundreds to thousands (see Fig. 1) almost anywhere in the observable Universe. Signals from higher mass systems will not significantly enter the frequency band, and systems with a total mass lower than $\sim 10^5 M_\odot$ will have signal amplitudes in LISA's band that quickly become too low to be observable.

How many SMBBH events is LISA expected to see in a year, and of what kind? There are several possible SMBBH formation scenarios that are able to reproduce the measured optical luminosity function of active galactic nuclei in the redshift range $1 \lesssim z \lesssim 6$, but they differ in (i) the formation mechanism and masses of the ``seed'' black holes, as well as in (ii) the details of how accretion causes black holes to grow in time. For instance, Volonteri et al. [1,39,40] consider a scenario where light seed black holes (of a few hundred $M_\odot$) were produced as remnants of metal-free stars at $z \gtrsim 20$. Alternatively, gravitational instability of massive proto-galactic disks at $z \gtrsim 10$ could have led to the formation of much heavier seeds with masses $\sim 10^5 M_\odot$ [2]. Regardless of seed masses, the seeds may have grown by an accretion process in which infalling matter has a constant angular momentum direction, spinning up the black holes [3,4], or by chaotic accretion from a fragmented disc, causing much smaller spins [5].

The implications for LISA of these various scenarios were recently assessed by the LISA PE Taskforce [6]. Generally, scenarios with heavy seeds lead to several tens of mergers per year in LISA's past light cone, all of which will be detectable. If the seeds were smaller then the rate in the past light cone will be a factor of several larger, but LISA's sensitivity to light black hole coalescences is smaller; here too the number of *observed* mergers is a few tens per year. Whatever scenario, in the course of its lifetime LISA may see a few merger events that are close
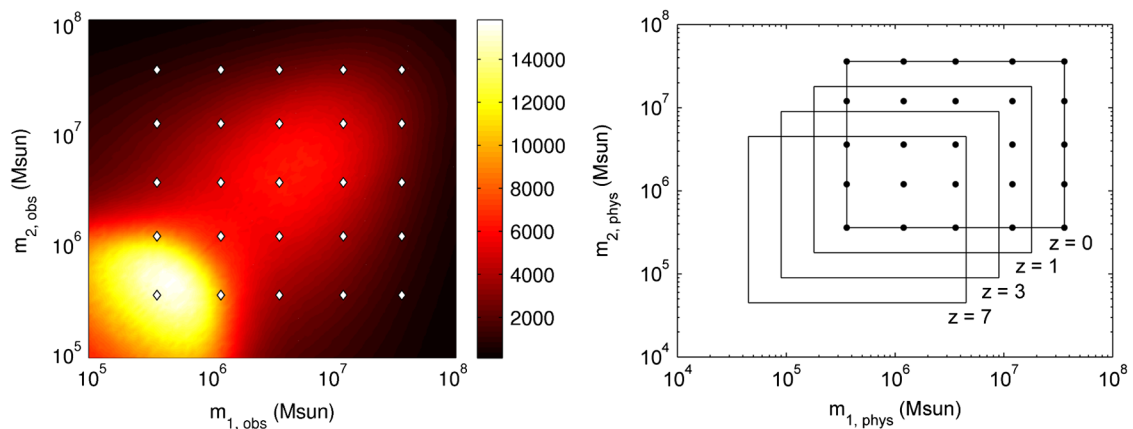

FIG. 1 (color online). Left: Median values of the measured signal-to-noise ratio (SNR$_{1\text{ Gpc}}$) from the inspiral phase of SMBBH systems at 1 Gpc, as a function of the observed masses of the individual black holes, obtained from 1000 Monte Carlo simulations over the sky location and orientation of the source. The quantity plotted is related to the observed SNR at any luminosity distance D_L as SNR$_{D_L}$ = SNR$_{1\text{ Gpc}} \times \frac{\text{Gpc}}{D_L}$. The superimposed diamonds represent the grid of observed mass cases considered to study parameter estimation and its implications in measuring the dark energy equation of state. Right: Representation of how the grid of observed masses in Fig. 1 (here as dots) translates into physical masses as we increase the redshift, z, of the source.

enough ($z \lesssim 2$) to be useful as standard sirens, but their expected masses differ depending on the scenario.

For this reason, in this work we did not focus attention on any particular part of the mass range and considered a uniform sampling of systems within LISA's mass reach. In particular, we have analyzed 15 different pairs of masses forming an almost uniform grid in the $\log m_1 - \log m_2$ plane that covers most[3] of the region of systems observable by LISA, as shown in Fig. 1: we consider all possible combinations of observed component masses $m_{1,2} = \{3.6 \times 10^5, 1.2 \times 10^6, 3.6 \times 10^6, 1.2 \times 10^7, 3.6 \times 10^7\}M_\odot$. As pointed out by a number of authors, e.g., [10,12,31], the observed SNRs and parameter estimation depend sensitively on the sky location and orientation of the source, so that MC simulations are called for if one wants to draw general conclusions about LISA's performance. Thus, in this work for each of our 15 pairs of masses, we have carried out 5000 MCs over $\{\cos\theta_N, \phi_N, \cos\theta_L, \phi_L\}$ drawn from a uniform distribution, computing in every case SNRs and parameter errors.

The luminosity distance, D_L, and redshift, z are extrinsic parameters in the problem. Since SNR, parameter uncertainties, and masses scale with these in simple ways, one can obtain a variety of results from calculations that were done with *fixed* values of D_L and z.[4]

Let us discuss the dependence of the results (SNRs and parameter errors) on the luminosity distance and redshift. First note that

(1) From conservation of energy, the amplitude of the gravitational-wave signal is inversely proportional to D_L.

(2) The frequency is redshifted because of the expansion of the Universe, which causes a blueshift in the observed masses relative to the physical ones: $m_{obs} = (1 + z)m_{phys}$, where m_{phys} stands for any intrinsic parameter with dimensions of mass.

Since the SNR and the Fisher information matrix are proportional to the signal amplitude and its square, respectively, we have[5]

$$\text{SNR} \propto \frac{1}{D_L}; \qquad \Delta D_L \propto D_L^2; \qquad \Delta\lambda \propto D_L, \qquad (3.1)$$

where λ is any parameter different from D_L. Thus, the quantities $\text{SNR} \times D_L$, $\Delta D_L/D_L^2$, and $\Delta\lambda/D_L$ are independent of D_L.

---

[3]The lower mass systems, despite their low amplitude, remain in the LISA band for many cycles, which makes the parameter estimation highly expensive in terms of computational time. For this reason we restricted ourselves to systems with masses higher than $3.6 \times 10^5 M_\odot$.

[4]Note that the output of a simulation is obtained without making any assumptions about the relationship between z and D_L.

[5]The error in the luminosity distance behaves differently because we are using the derivative with respect to the parameter we are varying.

On the other hand, the redshift experienced by any signal due to the expansion of the Universe translates into a shift in the physical masses. Thus, a single simulation made for some pair of observed masses, say $\{m_{1,obs}, m_{2,obs}\}$, will be representative of an infinite set of systems at different redshifts, z, with physical masses

$$m_{1,phys} = \frac{m_{1,obs}}{1 + z}, \qquad m_{2,phys} = \frac{m_{2,obs}}{1 + z}. \qquad (3.2)$$

In Fig. 1, the panel on the right illustrates how the observed masses in the left panel correspond to progressively lower physical masses as we consider sources at successively higher redshifts.

IV. IMPACT OF SOURCE LOCALIZABILITY ON PARAMETER ESTIMATION

Much of the literature on parameter estimation with LISA has used the restricted post-Newtonian waveform, which suggested that the position uncertainty would be too large and it would not be possible to find the host galaxy. But as pointed out by Sintes and Vecchio [15,16] and Hellings and Moore [17], and recently studied more thoroughly by Arun *et al.* [10], Trias and Sintes [12,13], and Porter and Cornish [14], the higher harmonics in the orbital frequency that will also be present in the signal, carry a significant amount of information, and including them in search templates can vastly improve parameter estimation. (This is also the case for ground-based detectors; see [29].) In particular, with the inclusion of subdominant signal harmonics, in many cases the uncertainty in sky position decreases dramatically, so that host identification becomes possible, allowing for accurate measurement of w, as shown in [10,11]. However, in the latter papers only a small number of example systems were considered. In the present work we aim to sample the parameter space far more thoroughly, enabling a much more detailed assessment of what might be possible.

If the host galaxy of an inspiral event can be found, then the sky position will be known with essentially no error. One would then match filter the signal against a template family with fixed values for θ_N and ϕ_N. This will help in removing the correlation between (θ_N, ϕ_N) and D_L, resulting in a smaller uncertainty in the estimation of the luminosity distance than before [11]. The distance error ΔD_L resulting from this smaller Fisher matrix is what determines the error on the dark energy equation-of-state parameter w [18].

The source localizability criterion that we consider in this paper is explained in next section, but first we are interested in the impact of the localization on the other parameters associated with inspiral events. Figure 2 and Table I show how knowledge of sky position improves the estimation of the unit normal to the inspiral plane (where $\Delta\Omega_L$ is the solid angle subtended by the two-dimensional uncertainty ellipse on the unit sphere), the luminosity

distance D_L, the coalescence time t_C, the phase at coalescence ϕ_C, the chirp mass $\mathcal{M}$, and the reduced mass μ. In these figures, we only consider "localizable" systems, consisting in a certain fraction (represented in Fig. 3) of the total.

We see the following trends:

(1) Knowing sky position has a bigger effect on light systems than on heavy ones. Heavier systems deposit less power into LISA's band and have a smaller SNR. In that case, our localizability requirement can only be fulfilled by systems where the correlations between parameters were already relatively small to begin with, so that parameter estimation would already have been good beforehand. Adding the information on sky position then will not lead to significantly more improvement.

(2) Symmetric systems show more improvement in parameter estimation when sky location is known than asymmetric ones. Indeed, the odd harmonics are all proportional to the difference between component masses $(m_1 - m_2)$, so that they are absent for symmetric systems. For asymmetric systems, the presence of the odd harmonics helps break degeneracies, and adding sky position information again does not lead to great improvement.

The improvements in the estimation of chirp mass and reduced mass are modest; depending on the system, the gains are between a fraction of a percent and 10% (for $\mathcal{M}$) or 14% (for μ). Much greater improvements can be seen in the measurement of the luminosity distance and the ori-

entation of the inspiral plane [i.e., the unit vector determined by (θ_L, ϕ_L)], as these are much more strongly correlated with sky position. The great accuracy in the determination of D_L (typically a fraction of a percent even for quite massive systems) will translate into excellent estimation of w, if weak lensing can be subtracted, as we shall see in the next sections.

V. COSMOLOGY AND MEASUREMENT OF DARK ENERGY

As argued in [9,41], by treating SMBBH as *standard sirens*, LISA could play a role in studying the physical nature of dark energy. From the gravitational-wave signal itself one can measure the luminosity distance D_L with good accuracy, but not the redshift. However, the amplitude and phase modulations induced in the observed gravitational waveform due to LISA's motion around the Sun allow for a determination of the source's position in the sky. If the error ellipse associated with the sky position measurement is small enough that it contains a sufficiently small number of galaxies or galaxy clusters, then it may be feasible to identify the host galaxy, possibly with the help of an electromagnetic counterpart to the inspiral event. In that case a redshift z can be obtained. Now, the relationship between D_L and z depends sensitively on cosmological parameters such as H_0, Ω_M, Ω_{DE}, and w—respectively, the Hubble parameter at the current epoch, the matter and dark energy density (normalized by the critical density), and the dark energy equation-of-state parameter. Hence, separate
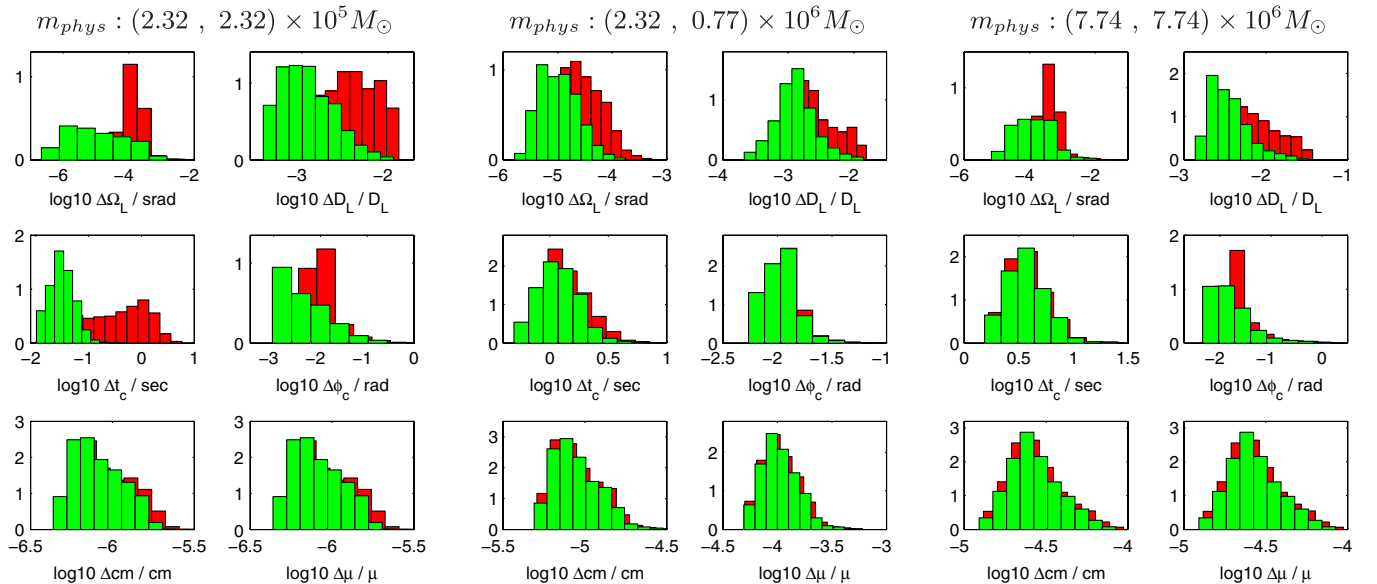

FIG. 2 (color online). Examples of distribution of errors on different parameters before (histograms in the back) and after (front histograms) fixing the sky location angles for three different combinations of masses: light and symmetric (left), intermediate and asymmetric (middle), and heavy and symmetric (right). $\Delta\Omega_L$, the error on the orientation of the orbital plane, is defined analogously to $\Delta\Omega_N$ [Eq. (5.2)]. We are assuming a fiducial luminosity distance of $D_L = 3$ Gpc ($z_0 = 0.55$), and we only consider the localizable systems for this case.

TABLE I. Improvement factors of the errors on different parameters after fixing the sky location angles for the localizable systems at $z_0 = 0.55$. In particular, the quoted numbers represent the ratios between the median values of the error distributions before and after fixing the sky location. Note that these are independent of D_L. We provide the results for six physical parameters and 15 choices of observed component mass pairs. The way the values are arranged corresponds to the location of the analyzed systems in the $\log(m_1) - \log(m_2)$ plane as in Fig. 3.

$\Delta\Omega_L$

				1.533
			3.471	2.179
		4.846	2.947	2.173
	3.581	2.906	2.655	1.722
14.871	5.937	2.952	2.135	1.279

$\Delta D_L / D_L$

				1.342
			1.980	1.432
		2.428	1.723	1.507
	1.960	1.753	1.565	1.411
3.644	2.380	1.750	1.356	1.202

Δt_C

				1.000
			1.019	1.138
		1.495	1.038	1.005
	2.963	1.146	1.004	1.002
15.564	1.982	1.150	1.005	1.005

$\Delta\phi_C$

				1.055
			1.399	1.153
		1.756	1.024	1.004
	1.344	1.026	1.002	1.002
2.830	1.008	1.010	1.004	1.007

$\Delta\mathcal{M}/\mathcal{M}$

				1.000
			1.006	1.099
		1.021	1.031	1.004
	1.029	1.011	1.006	1.002
1.055	1.015	1.010	1.005	1.006

$\Delta\mu/\mu$

				1.000
			1.006	1.141
		1.021	1.033	1.004
	1.029	1.009	1.002	1.003
1.055	1.013	1.003	1.005	1.006

measurements of the distances and redshifts to four or more sources would constrain these parameters.

For the purposes of this paper we assume a spatially flat Friedman-Lemaître-Robertson-Walker (FLRW) universe with constant w. In that case, the relationship between the luminosity distance D_L and redshift z is given by

$$D_L(z) = \frac{(1+z)}{H_0} \int_0^z \frac{dz'}{[\Omega_M(1+z')^3 + \Omega_{DE}(1+z')^{3(1+w)}]^{1/2}}. \quad (5.1)$$

In principle, a measurement of the cosmological parameters could proceed as follows. Imagine that a number of SMBBH inspiral events have been found in LISA data, and that their host galaxy has been identified. The redshifts z can then be determined with negligible error. From the gravitational-wave signals themselves, the luminosity distances could be extracted. A fit of D_L as a function of z using the expression (5.1) would then allow us to deduce the values of H_0, Ω_M, Ω_{DE}, and w. In practice, however, there may not be a large enough number of sources for which the sky position can be determined sufficiently well to allow the identification of the host galaxy, in which case it will be impracticable to constrain all four cosmological parameters at the same time.

In this paper we consider an illustrative example. We will assume that we only have access to a single inspiral event, which will be used to estimate one cosmological parameter, w in our case; the other parameters will be considered known with negligible errors. Such an observation would complement the estimation of $(H_0, \Omega_M, \Omega_{DE}, w)$ obtained by other means, e.g., via gravitational-wave observations of other LISA sources such as the extreme mass ratio inspirals (EMRIs) [42], or via the observations of stellar mass compact binaries with ground-based detectors like the Advanced LIGO [43] or the Einstein Telescope [44]. The latter may see as many as 500 (stellar mass) inspiral events per year with identifiable electromagnetic counterparts, giving several thousands over a period of five years. From each of the signals a luminosity distance could be extracted, and the electromagnetic counterpart would allow us to find the host and obtain a value for redshift. Fitting the function $D_L(z)$ would then severely constrain at least a subset of the unknowns $(H_0, \Omega_M, \Omega_{DE}, w)$ [44]. Even without these other gravitational-wave measurements, by the time LISA is operational, all of the parameters (including w) may already have been measured with good accuracy through electromagnetic means, by continued studies of the cosmic microwave background, baryon acoustic oscillations, gravitational lensing, and a larger population of Type Ia supernovae [45]. What LISA can add, even if only one parameter is measured, is an important *consistency check*: gravitational-wave astronomy brings the unique benefit that cosmological parameters can be constrained without reference to a cosmic distance ladder. It is then natural not to make any *a priori* assumptions on w.

As explained in the previous section, we simulated a large number of instances of SMBBH inspirals, with different masses, sky positions, and orientations of the orbital plane relative to the observer. We aim to answer two questions:

(1) What fraction of these instances allows for identification of the host galaxy?

(2) For each of the events where the host can be found, how accurately can we measure w?

First, we need a criterion to discriminate between cases where the host can be identified and cases where it cannot. In order to do this, we define a fiducial cosmological model which we will use as a reference; say, a spatially flat FLRW universe with $H_0 = 75 \text{ km s}^{-1} \text{Mpc}^{-1}$, $\Omega_M = 0.27$, $\Omega_{DE} = 0.73$, and $w = -1$. Using this fiducial model, to the measured value of D_L we can associate a fiducial redshift value z_0. Deciding whether or not the host galaxy can be found will involve counting the number of galaxies or galaxy clusters in some volume error box around the approximate sky position and distance of the inspiral event. The error ellipse in the sky, $\Delta\Omega_N$, will provide one constraint in determining such an error box; one has

$$\Delta\Omega_N = 2\pi\sqrt{(\Delta\cos(\theta_N)\Delta\phi_N)^2 - \langle\delta\cos(\theta_N)\delta\phi_N\rangle^2}. \quad (5.2)$$

However, we are not allowed to also use the error in the determination of *distance*, as measuring w requires an *independent* determination of the luminosity distance and redshift. Instead, we will count how many galaxies or clusters there are in an error box determined by the sky position error ellipse $\Delta\Omega_N$, and a large redshift interval centered on the fiducial redshift z_0. For concreteness we take this interval to be $[0.8z_0, 1.2z_0]$. This is a generous choice: given the above values of $(H_0, \Omega_M, \Omega_{DE})$, to reconcile the measured D_L with a redshift that differs by 10% from our fiducial z_0 will typically require picking a value of w that lies far outside the existing bounds from WMAP and supernovae studies [10,11]. The sky position error $\Delta\Omega_N$ together with the redshift interval $[0.8z_0, 1.2z_0]$ will, through our fiducial cosmological model, imply a comoving volume ΔV_C in which to search for host galaxies:

$$\Delta V_C = \int_{0.8z_0}^{1.2z_0} dz' \frac{\Delta\Omega_N}{H_0} \frac{D_L^2(z')}{(1+z')^2}$$
$$\times \frac{1}{\sqrt{\Omega_M(1+z')^3 + \Omega_{DE}(1+z')^{3(1+w)}}}. \quad (5.3)$$

To arrive at an actual number of galaxies or galaxy clusters within the volume ΔV_C we need an estimate for the density of clusters.[6] This density is not known very well; here, we follow Bahcall *et al.* [46], who give $\rho_{clusters} \sim 2 \times$

$10^{-5}h^3 \text{ Mpc}^{-3}$, with h the Hubble parameter at the current epoch in units of $100 \text{ km s}^{-1} \text{ Mpc}^{-1}$. The number of clusters within our volume error box can then be estimated as $N_{clusters} \simeq \rho_{clusters}\Delta V_C$. If for a particular inspiral event $N_{clusters}$ turns out to be of order 1 then the host cluster can be found and a redshift value can be obtained. It could be that the host can be identified even when $N_{clusters} \gg 1$, as the binary SMBBH merger might be accompanied by a distinctive electromagnetic counterpart which could be found by future large survey instruments though electromagnetic counterparts [47,48]. Even so, we will take $N_{clusters} < 3$ to be our localizability criterion. Issues related to finite cluster size and identification of the actual host galaxy will be discussed below. At first instance one wants to identify the host cluster, and for that it will typically not be problematic if there are several clusters within the volume box. As an example, consider an inspiral at 3 Gpc, which in our fiducial cosmological model corresponds to $z = 0.55$. Suppose the volume box contains a few clusters with redshifts differing by 10%, e.g., imagine there is a potential host cluster at $z = 0.6$. Then in order to reconcile this slightly larger redshift with the measured distance, for the same values of H_0, Ω_M, and Ω_{DE} one would arrive at $w = -0.47$, a value that is strongly excluded by WMAP and supernovae studies.

When the host galaxy or galaxy cluster of an inspiral event can be found, we can assume that the sky position will be known with essentially no error,[7] which will allow us to recompute a reduced Fisher matrix removing the correlations between (θ_N, ϕ_N) and the other parameters. In particular, this will translate into an improvement in the estimation of D_L (see Table I), which is what determines the error on the equation-of-state parameter w [18].

Assuming that $(H_0, \Omega_M, \Omega_{DE})$ are known with sufficient accuracy that their uncertainties can be neglected, the error on w [10,11] will be given by two contributions: (a) the uncertainty in D_L from LISA observations (gravitational wave) and (b) the error on z from the identification of the host galaxy or galaxy cluster (galaxy cluster),

$$\Delta w = \left|\frac{\partial D_L}{\partial w}\right|^{-1} D_L \left[\left(\frac{\Delta D_{L,GW}}{D_L}\right)^2 + \left(\frac{1}{D_L}\frac{\partial D_L}{\partial z}\right)^2 \Delta z_{GC}^2\right]^{1/2}$$
$$= \left|\frac{\partial D_L}{\partial w}\right|^{-1} D_L \left[\left(\frac{\Delta D_{L,GW}}{D_L}\right)^2 + \left(\frac{\Delta D_{L,GW}}{D_L}\right)^2\right]^{1/2}. \quad (5.4)$$

The second contribution to Δw could be significant in the cases where the host galaxy cluster could be identified, but not the individual galaxy. Even then, since the typical radius of a galaxy cluster is 5 Mpc [49], the contribution

---

[6]We note that at redshifts $z \sim 1$ and beyond, galaxy clusters become increasingly ill-defined; we will merely use the number of clusters as a quantitative way of judging whether the host of an inspiral event will be identifiable.

[7]For systems at $z = 1$, LISA's sky resolution will be at best 10^{-4} srad [12], whereas the solid angle subtended by a galaxy cluster at the same redshift is at least 2 orders of magnitude smaller. Hence, for the purposes of Fisher matrix calculations, we can assume that the sky position has negligible error when the host cluster can be identified.

from this term will be 0.17%, 0.12%, and 0.08% for $z_0 = 0.55$, $z_0 = 0.7$ and $z_0 = 1$, respectively. This is smaller than or comparable to the distance error from LISA's noise, so that neglecting it would make a difference of at most $\sim\sqrt{2}$. In what follows, we will assume that the host galaxy can be identified (which may be possible with large survey instruments through electromagnetic counterparts [47,48]) and therefore we neglect the contribution from the size of the cluster; but in any case, the main conclusions of this article would be the same.

An important problem in determining distances (also in conventional astronomy) is that of weak lensing. As the waveform propagates through the matter distribution between the source and observer, its amplitude will suffer an overall amplification or deamplification, leading to an additional random error in the estimation of D_L. For the range of distances considered here, this error will be at the level of 3–5% [19]. This is substantive: at a distance of 3 Gpc (or $z_0 = 0.55$), a distance error of 4% will correspond to an uncertainty in w of 23%. However, it may be possible to largely remove the effect of weak lensing by mapping the mass distribution along the line of sight (see, e.g., Refs. [50,51]). In the next section we will see that, if left uncorrected, weak lensing will completely dominate

over uncertainties due to LISA's instrumental noise in the determination of w.

VI. RESULTS

We now discuss the results for the localizability of sources, and the values of Δw obtained from our Monte Carlo simulations.

The top panels of Fig. 3 show the percentages of "useful" systems, i.e., the fraction of simulated inspiral events for which the sky position error is sufficiently small that the host galaxy could be identified, by our criterion $N_{\text{clusters}} < 3$. Results are given for three choices of redshift: $z_0 = 0.55$, $z_0 = 0.7$, and $z_0 = 1$, which, in our fiducial model, correspond to $D_L = 3$ Gpc, $D_L = 4$ Gpc and $D_L = 6.3$ Gpc, respectively. Two trends can be seen:

(1) When the total mass is high, the termination frequency $2F_{\text{ISCO}}$ of the dominant harmonic will be low and the signal will have less power in LISA's frequency band, being "visible" only during the last orbits before merger. Both the low observed SNR (see Fig. 1) and the short time over which the signal is observed will lead to relatively poor parameter estimation.
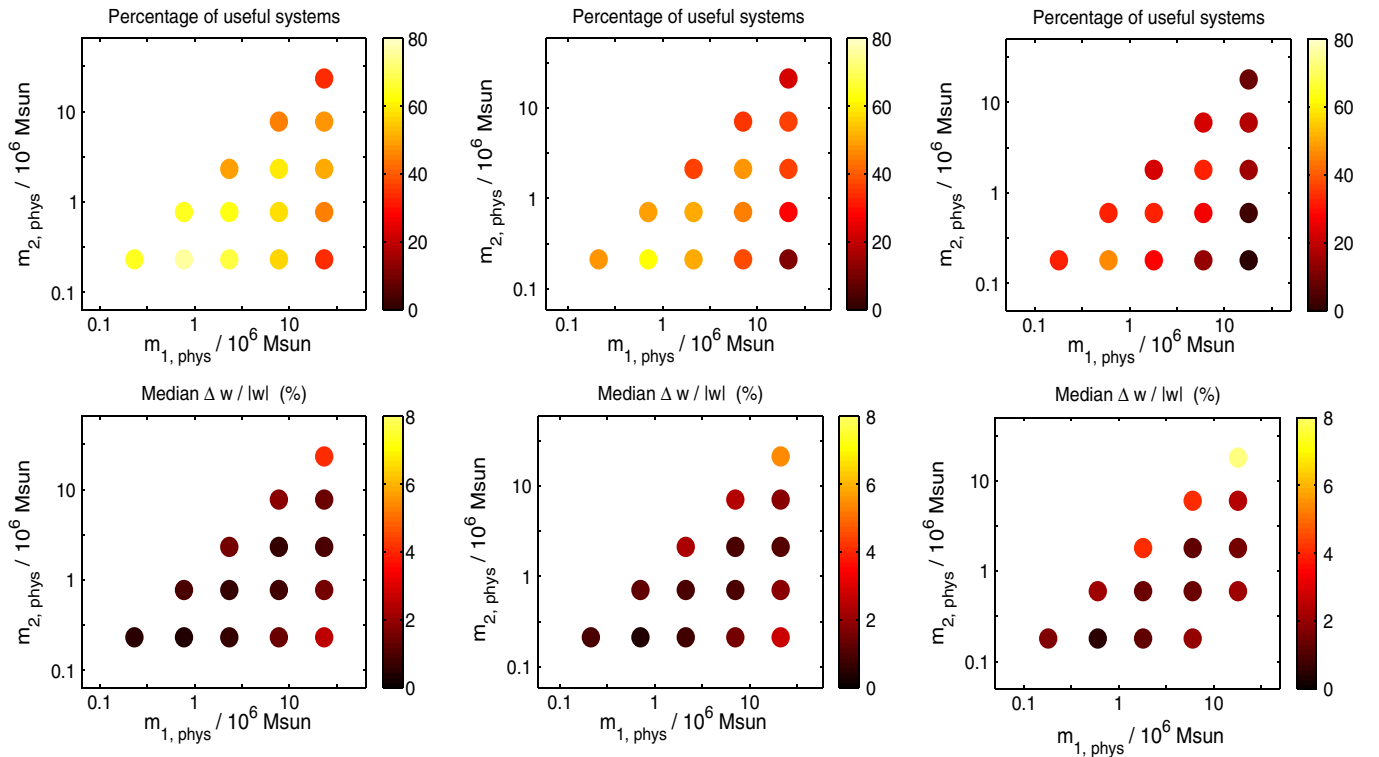

FIG. 3 (color online). Results for three choices of redshift: $z = 0.55$ (left column), $z = 0.7$ (middle column), and $z = 1$ (right column). In each column, the top plots show the fraction of inspiral events for which the host galaxy can be identified (by our criterion $N_{\text{clusters}} < 3$) for the various choices of component masses we considered. The bottom plots show the median uncertainties in the determination of w for the systems that allow for host determination and hence measurement of redshift. The masses are the physical ones.

(2) Parameter estimation will be worse for symmetric systems (i.e., $m_1 = m_2$); indeed, all odd harmonics of the orbital frequency are proportional to the mass difference $(m_1 - m_2)$ and hence will vanish in the equal mass case. The information they could otherwise have carried will then not be present.

For $z_0 = 0.55$, the largest fraction of useful systems is 76.5%, which occurs for light and very asymmetric systems with component masses $(1.2 \times 10^6, 3.6 \times 10^5)M_\odot$. The smallest fraction is 33.5%, for $(3.6 \times 10^7, 3.6 \times 10^5)M_\odot$; although these systems are even more asymmetric, they are too heavy to deposit much power in LISA's band. For $z_0 = 0.7$, the largest and smallest fractions of useful systems have dropped to 62.5% and 11.7%, respectively. For $z_0 = 1$ the analogous numbers are 46.0% and 0%, respectively. Indeed, for $(3.6 \times 10^7, 3.6 \times 10^7)M_\odot$, there are no systems in our simulated population for which $N_{\mathrm{clusters}} < 3$.

In the bottom panels of Fig. 3, the median values of $\Delta w/|w|$ are shown, for the useful systems where the host can be identified. Binaries with masses $(1.2 \times 10^6, 3.6 \times 10^5)M_\odot$, which gave the largest fraction of useful systems, also yield the smallest value for the median error on w: for $z_0 = 0.55$ this is $(\Delta w/|w|)_{\mathrm{median}} = 0.3\%$. Still for $z_0 = 0.55$, the largest median error, $(\Delta w/|w|)_{\mathrm{median}} = 4.1\%$, occurs for very heavy and symmetric systems with masses $(3.6 \times 10^7, 3.6 \times 10^7)M_\odot$. At $z_0 = 0.7$, the smallest and largest median errors on w are 0.4% and 5.5%, respectively. For $z_0 = 1$, and disregarding the mass pair for which there are no useful sources, the smallest and largest median errors on w are 0.6% and 8.2%, respectively.

So far we have discussed errors without taking weak lensing into account. In Figs. 4–6, we show the distributions of errors for each of the mass pairs separately, both with and without an additional 4% error folded into the distance error through a sum of quadratures, to mimic the effect of weak lensing. In all cases, even at $z_0 = 1$, LISA's instrumental errors tends to be far smaller than the combined instrumental and weak lensing errors. Indeed, a 4% error in D_{L} translates into an 18.5% to 23% error in w depending on redshift, and it is around these high values that the results for $\Delta w/|w|$ are sharply peaked when weak lensing is taken into account. This shows that, to make full use of LISA's potential, future studies should focus on correcting the weak lensing effect.

VII. CONCLUSIONS

LISA has the ability to approximately localize supermassive black hole binary coalescence events through modulation of the observed signal due to LISA's motion around the Sun. Electromagnetic follow-up observations could localize the source with negligible errors in the source's position in the sky and the redshift z of the host galaxy. From the gravitational waveform, the luminosity distance D_{L} can be inferred. The relationship between D_{L} and z depends sensitively on the past evolution of the Universe, which affects the gravitational-wave signal as it travels from the source to the detector over cosmological distances. Assuming that at sufficiently large scales the Universe is approximated well by a spatially flat FLRW model and that the Hubble constant, the density of matter and the density of dark energy are sufficiently well known, the observation of a single SMBBH event in LISA can be used to measure the equation-of-state parameter of dark energy w. Thus, such events can be used as standard sirens, similar to the standard candles of conventional cosmography, but with no need for calibration of distance though a cosmic distance ladder of different kinds of sources.

In [10,11], it was pointed out that inclusion of higher signal harmonics has a dramatic effect on source localization, making it more likely that we will be able to find the host galaxy for relatively close-by ($z \lesssim 1$) SMBBH coalescences; these are the ones needed for a good estimation of w. However, in those papers a relatively small number of systems were studied. Here we performed large-scale Monte Carlo simulations in order to exhaustively probe the relevant part of the parameter space. We considered 15 choices of observed component mass pairs, each being given 5000 possible sky positions and orientations, and the results were scaled to three different redshifts.

For each of the mass and redshift choices, we first computed how many systems would be localizable by the criterion that within a generous redshift interval there should at most be 3 possible host galaxies or galaxy clusters in the sky error ellipse. The fraction of localizable systems varies widely with total mass and mass ratio (light and asymmetric systems being better), but at our "intermediate" redshift of $z_0 = 0.7$ these were between 11.7% and 62.5%. We note that these numbers are likely to be on the conservative side. If a coalescence event is accompanied by a sufficiently obvious electromagnetic counterpart then our localizability criterion may be too strict. Furthermore, a more careful treatment of the coalescence process (inclusion of spins as well as merger and ringdown) would increase these percentages, as discussed below.

Next, we calculated uncertainties on w for those systems which passed our localizability requirement so that a redshift value would be available. Here too there is considerable dependence on the mass parameters; at $z_0 = 0.7$ the median errors came out to be between 0.4% and 5.5%.

The waveform model used here included higher signal harmonics; indeed, without these it becomes difficult to even approximately localize the source in the first place [10–13]. However, spins were ignored, which are also known to improve parameter estimation [52,53]. Recently Stavridis et al. have investigated how well w could be measured with the inclusion of spin-induced precession of the orbital plane, though without higher harmonics [24]; they found 1-σ uncertainties Δw that are

similar to the ones in the present work. Although higher harmonics and spins break the same degeneracies, no doubt some further improvements can be expected by combining the two. We also reiterate that, as in Ref. [24], we only looked at the inspiral signal. Inspiral-only position estimates can be improved once again if the merger and ringdown signal is taken into account. Babak *et al.* [21] and Thorpe *et al.* [22] made a start with this using waveforms from numerical relativity simulations, and an extensive study on localizability using semi-analytic (nonspinning) inspiral-merger-ringdown waveforms was performed by McWilliams *et al.* [23]. It would be interesting to see estimates for sky localizability and luminosity distance measurements with waveforms that have both higher har-

monics and spins in the inspiral part, and which incorporate merger and ringdown as well. The results concerning localizability of the source which we presented here may well be underestimates by factors of several.

As far as the luminosity distance is concerned, if we were only limited by LISA's instrumental noise and the confusion background due to Galactic white dwarf binaries, then here too there would be, with no doubt, room for improvement. However, measurements of D_L get "polluted" by weak lensing effects, which in turn affects the uncertainties on w. Recent work indicates that these effects can be substantially reduced by exploiting the brightness of galaxies as a tracer of the gravitational fields of matter along the line of sight [50], or through mapping shear and
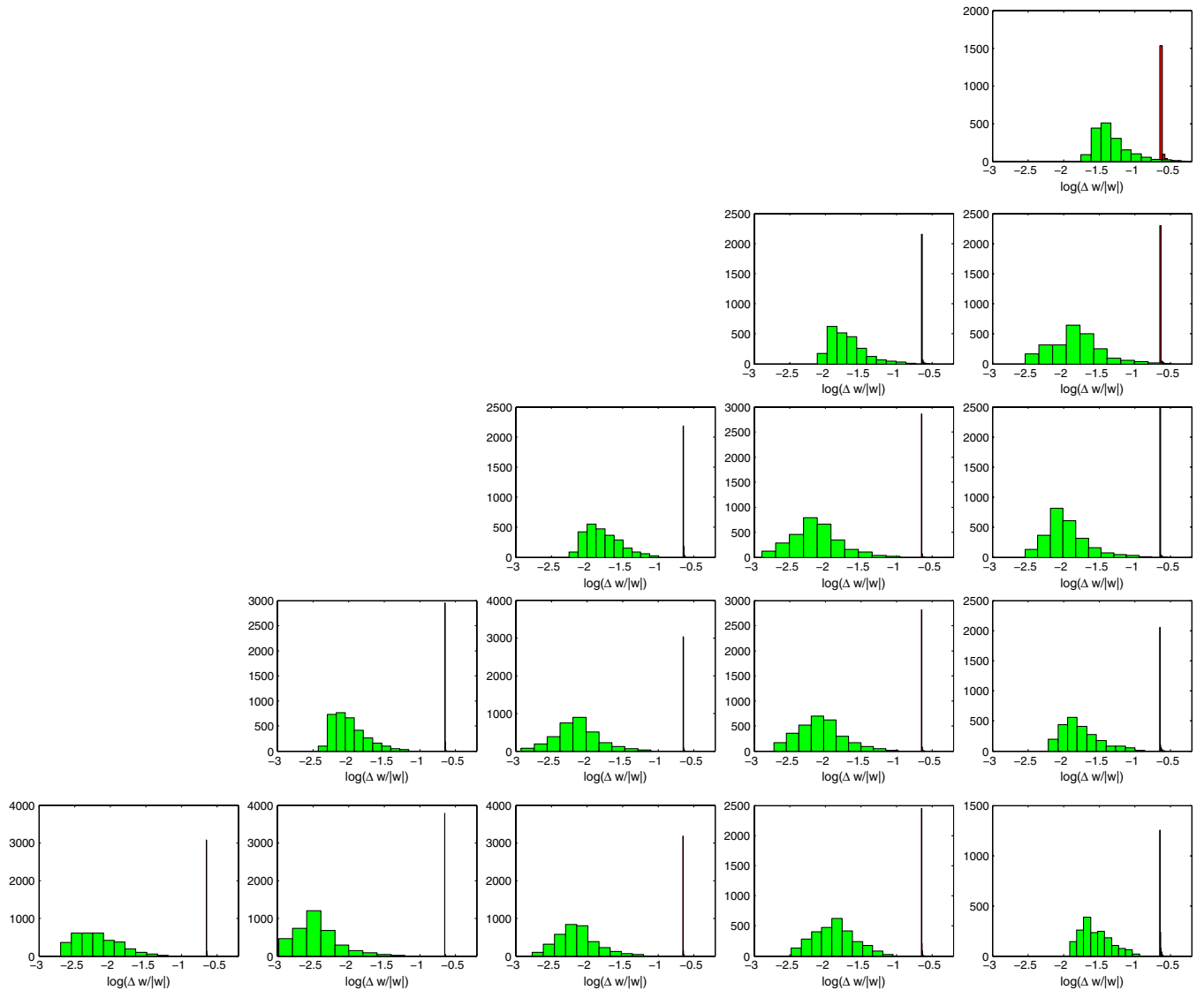

FIG. 4 (color online). Accuracies on the estimation of w for $z_0 = 0.55$ ($D_L = 3$ Gpc, according to our fiducial model). The way the plots are arranged corresponds to the location of systems in the $\log(m_1) - \log(m_2)$ plane as in Fig. 3. The light (green) distributions are without weak lensing; in the dark (red) distributions a 4% error in distance estimation has been folded in, as a heuristic way to account for weak lensing. Clearly, if the effects of weak lensing are not removed then they will dominate the uncertainty on w.

flexion of galaxy images [51]. With a deep and wide-field image of galaxies, as might be available with, e.g., Extremely Large Telescope [54] and Euclid [55] and with which one could construct a flexion map, one may be able to reduce the weak lensing error on D_L to about 1.5% in the redshift range $0.5 < z < 1$ [56]. At $z = 0.55$ this translates into an 8.5% uncertainty in w, which is competitive with electromagnetic measurements. By utilizing still higher-order effects in the apparent deformation of galaxies it may be possible to reduce this number a little further. Another idea would be to use high resolution cosmic microwave background maps to estimate weak lensing effects; it is not yet clear, however, how one might infer lensing effects at redshifts of $z \sim 1$ from such maps. The clear message of the results we have presented is that in order to use the full potential of LISA as a tool for cosmography, further in-depth studies are urgently needed on ways to correct for weak lensing.
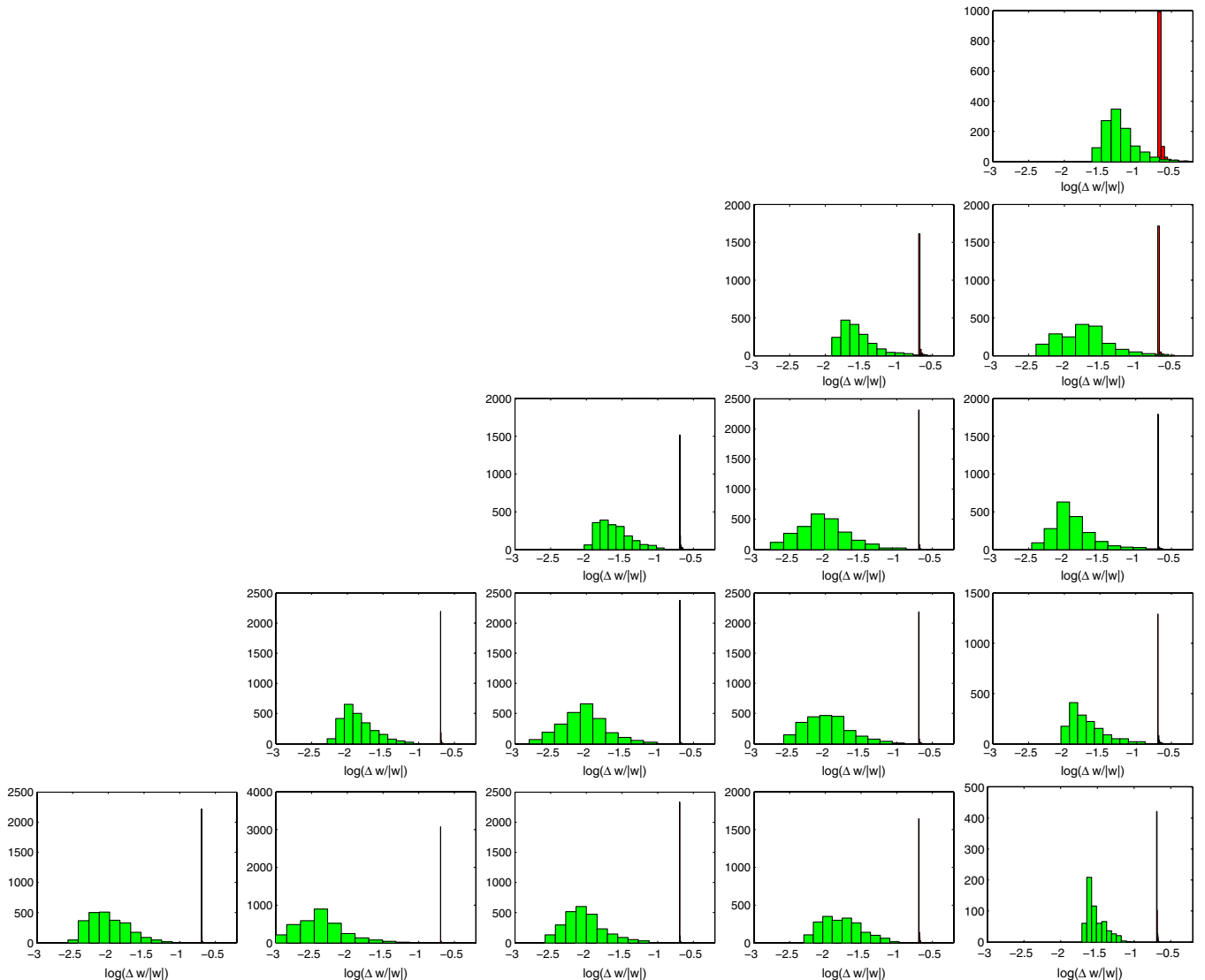
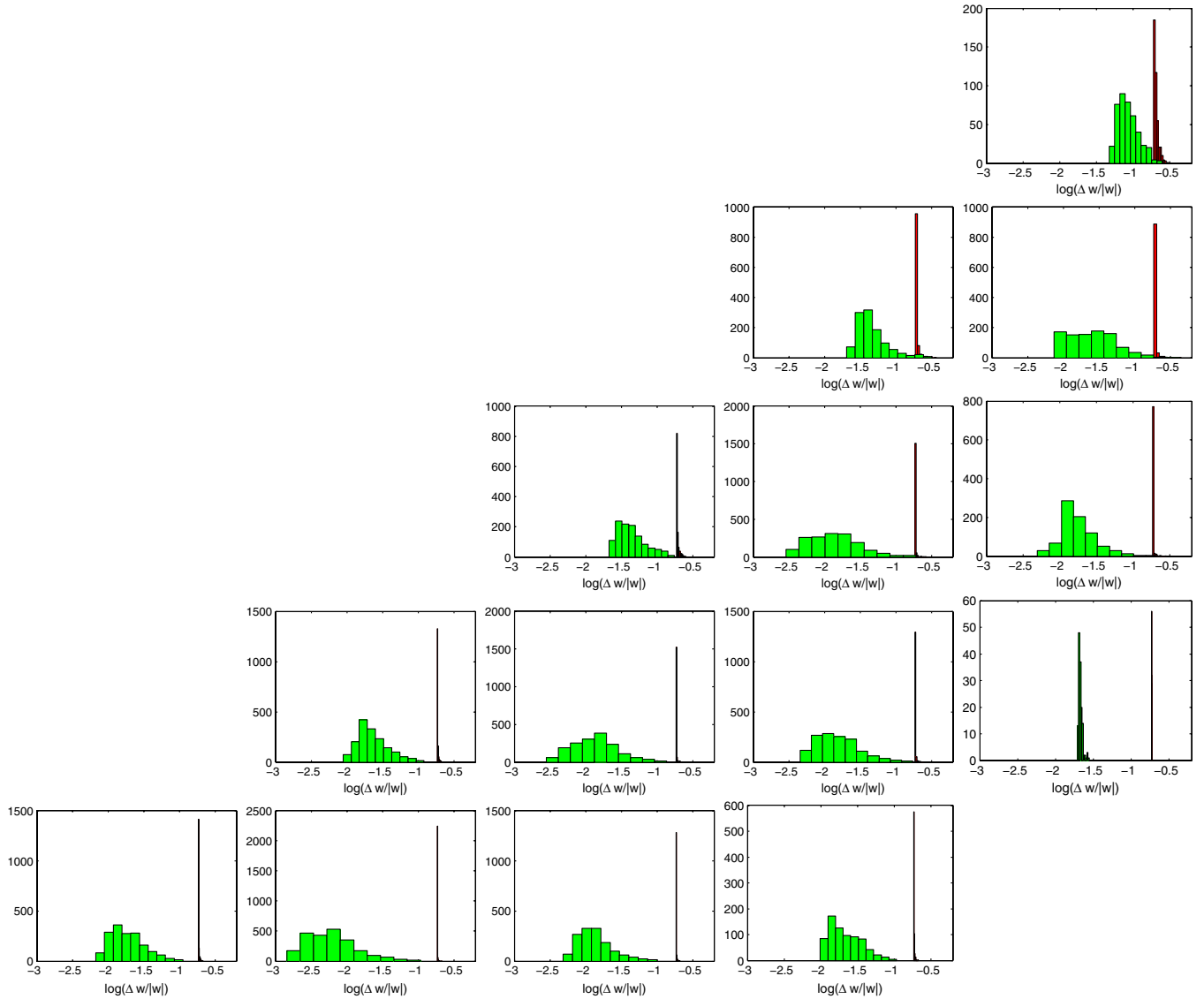FIG. 5 (color online). The same as in Fig. 4 but for $z_0 = 0.7$ ($D_L = 4$ Gpc).

FIG. 6 (color online).   The same as in Fig. 4 but for $z_0 = 1$ ($D_\mathrm{L} = 6.3$ Gpc).

[1] M. Volonteri, F. Haardt, and P. Madau, Astrophys. J. **582,** 559 (2003).

[2] M. C. Begelman, M. Volonteri, and M. J. Rees, Mon. Not. R. Astron. Soc. **370,** 289 (2006).

[3] J. M. Bardeen, Nature (London) **226,** 64 (1970).

[4] K. S. Thorne, Astrophys. J. **191,** 507 (1974).

[5] A. R. King and J. E. Pringle, Mon. Not. R. Astron. Soc. Lett. **373,** L90 (2006).

[6] K. G. Arun *et al.*, Classical Quantum Gravity **26,** 094027 (2009).

[7] B. F. Schutz, Nature (London) **323,** 310 (1986).

[8] D. E. Holz and S. A. Hughes, Classical Quantum Gravity **20,** S65 (2003).

[9] D. E. Holz and S. A. Hughes, Astrophys. J. **629,** 15 (2005).

[10] K. G. Arun *et al.* Phys. Rev. D **76,** 104016 (2007); **76,** 129903(E) (2007).

[11] K. G. Arun, C. K. Mishra, C. Van Den Broeck, B. R. Iyer, B. S. Sathyaprakash, and S. Sinha, Classical Quantum Gravity **26,** 094021 (2009).

[12] M. Trias and A. M. Sintes, Phys. Rev. D **77,** 024030 (2008).

[13] M. Trias and A. M. Sintes, Classical Quantum Gravity **25,** 184032 (2008).

[14] E. K. Porter and N. J. Cornish, Phys. Rev. D **78,** 064005 (2008).

[15] A. M. Sintes and A. Vecchio, in *Proceedings of the Third Amaldi Conference on Gravitational Waves*, edited by S. Meshkov, AIP Conf. Proc. No. 523 (AIP, New York, 2000), p. 403.

[16] A. M. Sintes and A. Vecchio, in *Rencontres de Moriond: Gravitational Waves and Experimental Gravity*, edited by J. Dumarchez (Frontieres, Paris, 2000).

[17] T. A. Moore and R. W. Hellings, Phys. Rev. D **65**, 062001 (2002).

[18] B. F. Schutz, Classical Quantum Gravity **26**, 094020 (2009).

[19] B. Kocsis, Z. Frei, Z. Haiman, and K. Menou, Astrophys. J. **637**, 27 (2006).

[20] L. Blanchet, Living Rev. Relativity **5**, 3 (2002).

[21] S. Babak, M. Hannam, S. Husa, and B. F. Schutz, arXiv:0806.1591.

[22] J. I. Thorpe, S. T. McWilliams, B. J. Kelly, R. P. Fahey, K. Arnaud, and J. G. Baker, Classical Quantum Gravity **26**, 094026 (2009).

[23] S. T. McWilliams, J. I. Thorpe, J. G. Baker, and B. J. Kelly, Phys. Rev. D **81**, 064014 (2010).

[24] A. Stavridis, K. G. Arun, and C. M. Will, Phys. Rev. D **80**, 067501 (2009).

[25] L. Blanchet, G. Faye, B. R. Iyer, and S. Sinha, Classical Quantum Gravity **25**, 165003 (2008).

[26] C. Cutler, Phys. Rev. D **57**, 7089 (1998).

[27] B. S. Sathyaprakash and S. V. Dhurandhar, Phys. Rev. D **44**, 3819 (1991).

[28] C. Van Den Broeck and A. S. Sengupta, Classical Quantum Gravity **24**, 155 (2007).

[29] C. Van Den Broeck and A. S. Sengupta, Classical Quantum Gravity **24**, 1089 (2007).

[30] L. Blanchet, G. Faye, B. R. Iyer, and B. Joguet, Phys. Rev. D **65**, 061501 (2002); **71**, 129902 (2005).

[31] K. G. Arun *et al.*, Phys. Rev. D **75**, 124002 (2007).

[32] L. S. Finn, Phys. Rev. D **46**, 5236 (1992).

[33] LISA Science Performance Evaluation (by Parameter Estimation), wikipage http://www.tapir.caltech.edu/dokuwiki/lisape:home.

[34] S. Babak *et al.* (Mock LISA Data Challenge Task Force Collaboration), Classical Quantum Gravity **25**, 114037 (2008).

[35] K. A. Arnaud *et al.*, Classical Quantum Gravity **24**, S551 (2007).

[36] G. Nelemans, L. R. Yungelson, and S. F. Portegies Zwart, Astron. Astrophys. **375**, 890 (2001).

[37] G. Nelemans, L. R. Yungelson, and S. F. Portegies Zwart,

[38] N. J. Cornish and T. B. Littenberg, Phys. Rev. D **76**, 083006 (2007).

[39] A. Sesana, M. Volonteri, and F. Haardt, Mon. Not. R. Astron. Soc. **377**, 1711 (2007).

[40] A. Sesana, M. Volonteri, and F. Haardt, Classical Quantum Gravity **26**, 094033 (2009).

[41] N. Dalal, D. E. Holz, S. A. Hughes, and B. Jain, Phys. Rev. D **74**, 063006 (2006).

[42] C. L. MacLeod and C. J. Hogan, Phys. Rev. D **77**, 043512 (2008).

[43] Samaya Nissanke, Scott A. Hughes, Daniel E. Holz, Neal Dalal, and Jonathan L. Sievers, arXiv:0904.1017v1.

[44] B. F. Schutz, B. S. Sathyaprakash, and C. Van Den Broeck, arXiv:0906.4151.

[45] A. Albrecht *et al.*, arXiv:astro-ph/0609591.

[46] N. Bahcall *et al.*, Astrophys. J. Suppl. Ser. **148**, 243 (2003).

[47] R. N. Lang and S. A. Hughes, Astrophys. J. **677**, 1184 (2008).

[48] B. Kocsis, Z. Haiman, and K. Menou, Astrophys. J. **684**, 870 (2008).

[49] D. W. Hogg, J. G. Cohen, and R. Blandford, Astrophys. J. **545**, 32 (2000).

[50] C. Gunnarsson, T. Dahlen, A. Goobar, J. Jonsson, and E. Mortsell, Astrophys. J. **640**, 417 (2006).

[51] C. Shapiro, D. Bacon, M. Hendry, and B. Hoyle, arXiv:0907.3635v1.

[52] A. Vecchio, Phys. Rev. D **70**, 042001 (2004).

[53] R. N. Lang and S. A. Hughes, Phys. Rev. D **74**, 122001 (2006); **77**, 109901(E) (2008).

[54] ELT Science Working Group, An Expanded View of the Universe: Science with the European Extremely Large Telescope, 2009, http://www.eso.org/sci/facilities/eelt/science/doc/.

[55] R. Laureijs *et al.*, ESA Science Requirements Document: (ref: DEM-SA-Dc-00001), 2009, http://sci.esa.int/science-e/www/object/index.cfm?fobjectid=42822.

[56] M. Hendry (private communication).

Mon. Not. Roy. Astron. Soc. **349**, 181 (2004).